N_2O_5 uptake onto saline mineral dust: a potential missing source of tropospheric $ClNO_2$ in inland China

Haichao Wang[1,7,#], Chao Peng[2,#], Xuan Wang[3,#], Shengrong Lou[4], Keding Lu[5], Guicheng Gan[6], Xiaohong Jia[1], Xiaorui Chen[5], Jun Chen[6], Hongli Wang[4], Shaojia Fan[1,7], Xinming Wang,[2,8,9] Mingjin Tang[2,8,9,*]

[1] School of Atmospheric Sciences, Sun Yat-sen University, Guangzhou, China

[2] State Key Laboratory of Organic Geochemistry, Guangdong Key Laboratory of Environmental Protection and Resources Utilization, and Guangdong-Hong Kong-Macao Joint Laboratory for Environmental Pollution and Control, Guangzhou Institute of Geochemistry, Chinese Academy of Sciences, Guangzhou, China

[3] School of Energy and Environment, City University of Hong Kong, Hong Kong SAR, China

[4] State Environmental Protection Key Laboratory of Formation and Prevention of the Urban Air Complex, Shanghai Academy of Environmental Sciences, Shanghai, China

[5] State Key Joint Laboratory of Environmental Simulation and Pollution Control, College of Environmental Sciences and Engineering, Peking University, Beijing, China

[6] Institute of Particle and Two-Phase Flow Measurement, College of Energy and Power Engineering, University of Shanghai for Science and Technology, Shanghai, China

[7] Guangdong Provincial Observation and Research Station for Climate Environment and Air Quality Change in the Pearl River Estuary, Key Laboratory of Tropical Atmosphere-Ocean System, Ministry of Education, Southern Marine Science and Engineering Guangdong Laboratory (Zhuhai), Zhuhai, China

[8] CAS Center for Excellence in Deep Earth Science, Guangzhou 510640, China

[9] University of Chinese Academy of Sciences, Beijing, China

[#]These authors contributed equally to this work

*correspondence: Mingjin Tang (mingjintang@gig.ac.cn)

Abstract

Nitryl chloride ($ClNO_2$), an important precursor of Cl atoms, significantly affects atmospheric oxidation capacity and O_3 formation. However, sources of $ClNO_2$ in inland China have not been fully elucidated. In this work, laboratory experiments were conducted to investigate heterogeneous reactions of N_2O_5 with eight saline mineral dust samples collected from different regions in China, and substantial formation of $ClNO_2$ was observed in these reactions. $ClNO_2$ yields, $\varphi(ClNO_2)$, showed large variations (ranging from <0.05 to ~0.77) for different saline mineral dust samples, depending on mass fractions of particulate chloride. In addition, $\varphi(ClNO_2)$ could increase, decrease or show insignificant change for different saline mineral dust samples when relative humidity (RH) increased from 18% to 75%. We further found that current parameterizations significantly overestimated $\varphi(ClNO_2)$ for heterogeneous uptake of N_2O_5 onto saline mineral dust. In addition, assuming a uniform $\varphi(ClNO_2)$ value of 0.10 for N_2O_5 uptake onto mineral dust, we used a 3-D chemical transport model to assess the impact of this reaction on tropospheric $ClNO_2$ in China, and found that weekly mean nighttime maximum $ClNO_2$ mixing ratios could have been increased by up to 85 pptv during a severe dust event in May 2017. Overall, our work showed that heterogeneous reaction of N_2O_5 with saline mineral dust could be an important source of tropospheric $ClNO_2$ in inland China.

1 Introduction

The formation of O_3 and secondary aerosols, two major air pollutants, is closely related to atmospheric oxidation processes (Lu et al., 2019). Primary pollutants emitted by natural and anthropogenic sources are oxidized by various oxidants to produce O_3 and secondary aerosols, affecting air quality and climate. Major tropospheric oxidants include OH radicals, NO_3 radicals and O_3, and in the last two decades Cl atoms have been proposed as an important oxidant (Saiz-Lopez and von Glasow, 2012; Simpson et al., 2015; Wang et al., 2019). Rate constants for reactions of certain volatile organic compounds (VOCs) with Cl atoms can be a few orders of magnitude larger than those reacting with OH radicals (Atkinson and Arey, 2003; Atkinson et al., 2006); therefore, despite its lower concentrations in the troposphere, Cl can contribute significantly to atmospheric oxidation capacity in some regions (Saiz-Lopez and von Glasow, 2012; Simpson et al., 2015; Wang et al., 2019). For example, a modeling study (Sarwar et al., 2014) suggested that including Cl chemistry in the model could enhance oxidative degradation of VOCs by >20% in some locations.

One major source of tropospheric Cl atoms is daytime photolysis of $ClNO_2$ (Thornton et al., 2010; Simpson et al., 2015), which is formed in heterogeneous reaction of N_2O_5 with chlorine-containing particles (R1) at nighttime (Osthoff et al., 2008; Thornton et al., 2010):

$$N_2O_5(g) + Cl^-(aq) \rightarrow \varphi ClNO_2(g) + (2-\varphi)NO_3^-(aq) \qquad (R1)$$

The uptake coefficient, $\gamma(N_2O_5)$, and the $ClNO_2$ yield, $\varphi(ClNO_2)$, both depend on relative humidity (RH), aerosol composition and mixing state, and etc. (Bertram and Thornton, 2009; Ryder et al., 2014; Mitroo et al., 2019; McNamara et al., 2020; Yu et al., 2020). Cl atoms produced by $ClNO_2$ photolysis can effectively enhance atmospheric oxidation (Le Breton et al., 2018; Wang et al., 2019) and thus increase concentrations of O_3 and OH radicals during the day (Simon et al., 2009;

Riedel et al., 2014; Sarwar et al., 2014; Tham et al., 2016; Wang et al., 2016). In addition, $ClNO_2$ is an important temporary reservoir of NO_x at night and releases NO_2 during the daytime via photolysis, thereby further affecting daytime photochemistry.

Sea spray aerosol is the most important source of particulate chloride (Cl^-), and $ClNO_2$ is expected to be abundant at marine and coastal regions impacted by anthropogenic emissions. High levels of $ClNO_2$ have been observed at various marine and coastal regions over the globe (Simon et al., 2009; Riedel et al., 2012; Tham et al., 2014; Young et al., 2014; Wang et al., 2016; Osthoff et al., 2018; Wang et al., 2020a; Yu et al., 2020). In addition, many studies (Thornton et al., 2010; Mielke et al., 2011; Phillips et al., 2012; Riedel et al., 2013; Bannan et al., 2015; Faxon et al., 2015; Wang et al., 2017b; Wang et al., 2017c; Tham et al., 2018; Wang et al., 2018) have also reported significant amounts of $ClNO_2$ at various continental sites with limited marine influence. For example, $ClNO_2$ concentrations reached 4 ppbv in the summer of North China Plain (Tham et al., 2016). These observations imply the importance of other sources for aerosol chloride, such as coal combustion (Eger et al., 2019), biomass burning (Ahern et al., 2017), waste incineration (Bannan et al., 2019), and snow-melting agent application (Mielke et al., 2016; McNamara et al., 2020).

In addition to insoluble minerals (e.g., quartz, feldspar, clay and carbonate), mineral dust aerosols emitted from saline topsoil in arid and semi-arid regions may contain significant amounts of soluble materials such as chloride and sulfate (Gillette et al., 1992; Abuduwailli et al., 2008; Zhang et al., 2009; Wang et al., 2012; Jordan et al., 2015; Frie et al., 2017; Gaston et al., 2017; Tang et al., 2019; Gaston, 2020). As elemental and mineralogical compositions are different for conventional and saline mineral dust, they would differ significantly in physicochemical properties and impacts on atmospheric chemistry and climate. For example, hygroscopicity and cloud condensation nuclei (CCN) activities of saline mineral dust can be much higher than conventional

mineral dust (Pratt et al., 2010; Gaston et al., 2017; Tang et al., 2019; Zhang et al., 2020). Recent laboratory studies (Mitroo et al., 2019; Royer et al., 2021) found that heterogeneous reactions of N_2O_5 with saline mineral dust originating from western and southwestern USA can be very effective and produce significant amounts of $ClNO_2$. Large variations in $\gamma(N_2O_5)$ and $\varphi(ClNO_2)$ were reported (Mitroo et al., 2019; Royer et al., 2021), depending on RH as well as chemical and mineralogical contents of saline mineral dust samples.

A very recent study (Wu et al., 2020) showed that N_2O_5 uptake onto saline mineral dust contributed significantly to particulate nitrate formation during a dust storm event in Shanghai, China. One may further expect that it may have a profound effect on $ClNO_2$, especially considering that vast areas in China are heavily affected by both mineral dust and NO_x. Nevertheless, heterogeneous formation of $ClNO_2$ from N_2O_5 uptake onto saline mineral dust in other regions rather than USA has not been explored. In order to provide key parameters required to assess the potential of saline mineral dust as a $ClNO_2$ source in China, we conducted a series of laboratory experiments to investigate $ClNO_2$ formation in heterogeneous reaction of N_2O_5 with several saline mineral dust samples collected from different regions in China. In addition to difference in source regions, saline mineral dust samples examined in our work have substantial variations in composition and mineralogy, enabling us to examine the effects of particle composition and water content on $ClNO_2$ production. In order to better understand variations of $ClNO_2$ yields with RH and samples, we experimentally measured mass hygroscopic growth factors of the eight samples examined, while previous studies (Mitroo et al., 2019; Royer et al., 2021) used the thermodynamic model ISORROPIA-II (Fountoukis and Nenes, 2007) to predict particulate water contents. Based on our laboratory results, we further use a 3-D chemical transport model (GEOS-Chem) to assess

the impacts of $ClNO_2$ produced from N_2O_5 uptake onto mineral dust on $ClNO_2$ and O_3 in China during a major dust event which occurred in May 2017.

2 Methodology

2.1 Characterization of saline mineral dust samples

Eight saline mineral dust samples, originating from five different provinces in northern China (including Ningxia, Xinjiang, Shandong, Inner Mongolia and Shaanxi), were examined in this work, and full information of these samples can be found elsewhere (Tang et al., 2019). Table 1 summarizes key information of these samples. According to their chloride contents, the eight samples were classified into three categories, including two high chloride samples (H1 and H2), four medium chloride samples (M1, M2, M3 and M4) and two low chloride samples (L1 and L2).

Our previous work (Tang et al., 2019; Zhang et al., 2020) measured mass hygroscopic growth factors of the eight samples at 0-90% RH with a RH resolution of 10%, using a vapor sorption analyzer (Gu et al., 2017). As the highest RH at which heterogeneous reaction of N_2O_5 with saline mineral dust was conducted in our work was ~75%, we further measured mass growth factors of the eight samples at (75±2)% RH, and the results are also included in Table 1.

Table 1. Overview of mass fractions of major soluble ions and mass ratios of particulate water at (75±2)% RH to dry particles for the eight saline mineral dust samples examined in this work. Mass fractions of major soluble ions were reported previously (Tang et al., 2019), and particulate water contents at (75±2)% RH were measured by the present work.

category	sample [a]	sample [b]	Na^+	Cl^-	SO_4^{2-}	H_2O (75%)
High Cl^-	H1	NX	0.3537	0.3870	0.0958	1.3093
	H2	XJ-5	0.2407	0.2145	0.0973	1.7066

Medium Cl^-	M1	SD	0.0265	0.0508	0.0754	0.3911
	M2	XJ-4	0.0326	0.0341	0.0071	0.0428
	M3	IM-2	0.0471	0.0229	0.1413	0.2106
	M4	IM-3	0.1343	0.0095	0.3424	0.0174
Low Cl^-	L1	XJ-3	0.0239	0.0093	0.0497	0.0475
	L2	SX	0.0003	n.d.	n.d.	0.0126

[a]: sample names used in the present work; [b]:corresponding sample names used in our previous work (Tang et al., 2019).

2.2 Experimental apparatus

Figure 1 shows the experimental apparatus used to study heterogeneous interactions of N_2O_5 with saline mineral dust. It mainly consists of three parts: 1) N_2O_5 generation, 2) gas-particle interaction, and 3) detection of N_2O_5 and $ClNO_2$.

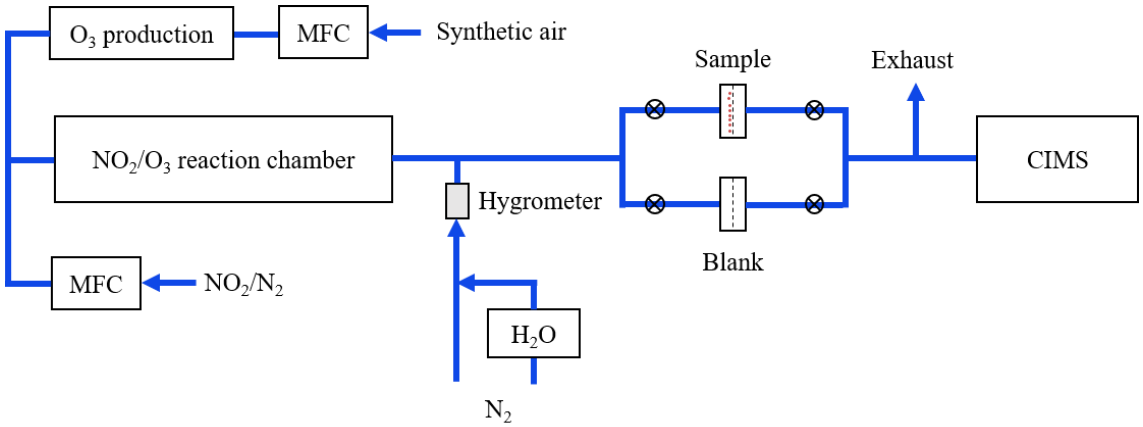

Figure 1. Schematic diagram of the experimental apparatus.

2.2.1 N_2O_5 generation

In our work, N_2O_5 was generated via oxidation of NO_2 by O_3. As shown in Figure 1, a synthetic air flow (30 mL/min) was passed over a Hg lamp to produce O_3 via O_2 photolysis at 184.95 nm. The photolysis module was stabilized at 35±0.2 °C using a Peltier cooler controlled by a Proportion Integration Differentiation (PID) algorithm, in order to give stable O_3 output. The

O_3/air flow was then mixed with a NO_2 flow (80 mL/min, 10 ppmv in synthetic air) in a temperature-stabilized PFA reactor with a residence time of ~70 s to produce N_2O_5. After exiting the PFA reactor, the flow (110 mL/min) was then diluted with a humidified nitrogen flow (2500 mL/min), and RH of the humidified nitrogen flow was monitored using a hygrometer. The final flow had a total flow rate of 2610 mL/min.

2.2.2 Heterogeneous interactions

As shown in Figure 1, the mixed flow (2610 mL/min) could be directed through a blank PTFE membrane filter (47 mm, Whatman, USA) housed in a PFA filter holder, and in this case initial N_2O_5 and $ClNO_2$ concentrations were measured; in our experiments, initial N_2O_5 concentrations were in the range of 0.4-1.0 ppbv. Alternatively, the flow could also be passed through a PTFE filter loaded with saline mineral dust, and thus N_2O_5 and $ClNO_2$ concentrations after heterogeneous reaction with saline mineral dust loaded on the filter were measured. During our experiments, the flow could be switched back to pass through the blank filter in order to check whether the initial N_2O_5 and $ClNO_2$ concentrations were stable.

Saline mineral dust particles were loaded onto PTFE filters using the method described in our previous study (Li et al., 2020; Jia et al., 2021). In brief, 10 mL particle/ethanol mixture was transferred onto a PTFE filter, and after ethanol was evaporated a relatively uniform particle film, as revealed by visual inspection, was formed on the filter. PTFE filters were weighted before and after being loaded with particles, in order to determine the mass of particles loaded onto these filters. In our work, the mass of particles on filters were in range of 0.6-7.3 mg.

2.2.3 Detection of N_2O_5 and $ClNO_2$

After exiting one of the two filters, a flow of 2200 mL/min was sampled into a time-of-flight chemical ionization mass spectrometry (TOF-CIMS) to measure N_2O_5 and $ClNO_2$ concentrations,

and the remaining flow (~400 mL/min) went into the exhaust. The CIMS instrument has been detailed previously (Kercher et al., 2009; Wang et al., 2016). In brief, N_2O_5 and $ClNO_2$ were detected as $I(N_2O_5)^-$ and $I(ClNO_2)^-$ clusters at 235 and 208 m/z (R2a, R2b) using I^- as the reagent ion, and a soft X-ray device (Hamamatsu, Soft X-Ray 120^o) was employed to generate I^- from CH_3I/N_2. CIMS was calibrated before and after our experiments which lasted for ~1 month, and further details on calibration can be found in the Appendix. The detection limits were 2 pptv for N_2O_5 and 3 pptv for $ClNO_2$, calculated as four times of standard deviations (4 σ) when measuring blank samples with 1 min average, and the accuracy was estimated to be ~25%.

$$N_2O_5 + I^- \rightarrow I(N_2O_5)^- \qquad \text{(R2a)}$$

$$ClNO_2 + I^- \rightarrow I(ClNO_2)^- \qquad \text{(R2b)}$$

2.3 Model description

We use GEOS-Chem (version 12.9.3) to quantify the effects of $ClNO_2$ formation due to heterogeneous reaction of N_2O_5 with saline dust in China. The model, which includes a detailed representation of coupled ozone-NO_x-VOCs-aerosol-halogen chemistry (Wang et al., 2021), is driven by MERRA2 (the Modern-Era Retrospective Analysis for Research and Applications, Version 2) assimilated meteorological fields from the NASA Global Modeling and Assimilation Office (GMAO) with native horizontal resolution of 0.25^o×0.3125^o and 72 vertical levels from the surface to the mesosphere. Our simulation was conducted over East Asia (60°-150°E, 10°S-55°N) at the native resolution with dynamical boundary conditions from a 4°×5° global simulation. Anthropogenic emissions in China are based on the Multiresolution Emission Inventory for China (MEIC) (Zheng et al., 2018) and an inventory of HCl and fine particulate Cl^- in China (Fu et al., 2018). Natural dust emissions are calculated based on Ridley et al. Ridley et al. (2013). A more detailed description of the model and emissions can be found elsewhere (Wang et al., 2020b).

For N_2O_5 uptake onto aqueous aerosols, the parameterization in our previous study (Wang et al., 2020b) for $\gamma(N_2O_5)$ and $\varphi(ClNO_2)$, which are based on a detail evaluation of different model parameterizations by previous work (McDuffie et al., 2018a; McDuffie et al., 2018b), is used in this study, and more details can be found in the supplement. For N_2O_5 uptake on dust aerosol, $\gamma(N_2O_5)$ is always assumed to be 0.02, as recommended previously (Crowley et al., 2010; Tang et al., 2017), and $\varphi(ClNO_2)$ is assumed to be 0 in the standard case, i.e., no $ClNO_2$ is produced in heterogeneous reaction of N_2O_5 with mineral dust.

3 Results and discussion

Figure 2a shows changes in N_2O_5 and $ClNO_2$ concentrations during an experiment in which heterogeneous reaction of N_2O_5 with sample H1 at 37% RH was studied. As shown in Figure 2a, when the mixed flow was passed through the blank filter (0-10 min), N_2O_5 concentrations were measured to be ~350 pptv and $ClNO_2$ was below the detection limit. The mixed flow was then passed through the particle-loaded filter at ~10 min in order to initiate heterogeneous reaction of N_2O_5 with sample H1, and significant decrease in N_2O_5 concentrations (from ~350 to ~150 pptv) and increase in $ClNO_2$ concentrations (from almost 0 to ~150 pptv) were observed, suggesting that heterogeneous interaction with sample H1 substantially consumed N_2O_5 and generated $ClNO_2$. In order to check if initial N_2O_5 and $ClNO_2$ concentrations were stable, during our experiments the mixed flow was switched back to pass through the blank filter from time to time (e.g., at around 40, 75 and 105 min for the experiment displayed in Figure 2a). Indeed, initial N_2O_5 and $ClNO_2$ concentrations were constant in our experiments, with another two examples shown in Figures 2b and 2c.

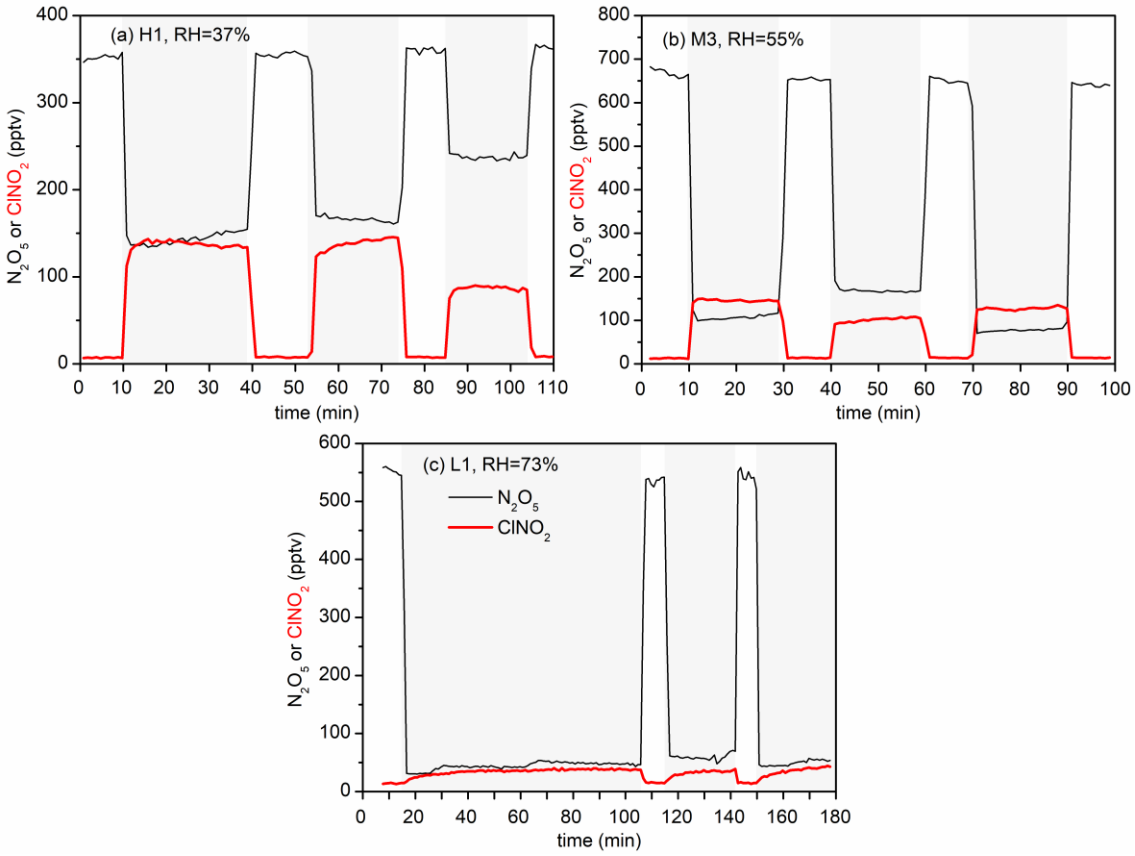

Figure 2. Time series for measured N_2O_5 and $ClNO_2$ concentrations after the mixed flow was passed through the blank filter or the particle-loaded filter: a) H1, 37% RH; b) M3, 55% RH; c) L1, 73% RH. Periods in which the mixed flow was passed through the particle-loaded filter was shadowed with gray.

Figures 2b and 2c show time series of measured N_2O_5 and $ClNO_2$ concentrations in another two experiments, suggesting that heterogeneous reaction with sample M3 and L1 also led to substantial removal of N_2O_5. However, much less $ClNO_2$ was produced for sample M3 and L1, when compared to sample H1 (Figure 2a). The decrease in N_2O_5 concentrations, $\Delta[N_2O_5]$, and the increase in $ClNO_2$ concentrations, $\Delta[ClNO_2]$, can be used to calculate $ClNO_2$ yields, $\varphi(ClNO_2)$, according to Eq. (1).

$$\varphi(\mathrm{ClNO_2}) = \frac{\Delta[\mathrm{ClNO_2}]}{\Delta[\mathrm{N_2O_5}]} \qquad (1)$$

In this work we measured $\varphi(\mathrm{ClNO_2})$ for heterogeneous reaction of N_2O_5 with eight different saline mineral dust samples at four RH, and each experiment was repeated at least three times. It should be mentioned that during each experiment the measured $\varphi(\mathrm{ClNO_2})$ did not vary significantly with time, and therefore an average value of $\varphi(\mathrm{ClNO_2})$ was reported for each experiment. Table 2 summarizes measured $\varphi(\mathrm{ClNO_2})$ for the eight samples at different RH, and the results are further discussed in the following sections.

Table 2. Measured $ClNO_2$ yields for heterogeneous uptake of N_2O_5 onto saline mineral dust samples at different RH. All the errors given in this work are standard deviations. The uncertainty of RH was ±2%.

sample	18% RH	36% RH	56% RH	75% RH
H1	0.402±0.138	0.663±0.039	0.774±0.028	0.697±0.311
H2	0.560±0.046	0.474±0.026	0.494±0.042	0.378±0.069
M1	0.271±0.038	0.271±0.030	0.418±0.053	0.543±0.086
M2	0.166±0.018	0.246±0.041	0.316±0.046	0.418±0.052
M3	0.223±0.061	0.251±0.050	0.211±0.025	0.120±0.050
M4	0.179±0.075	0.133±0.007	0.205±0.021	0.181±0.044
L1	0.037±0.006	0.030±0.015	0.045±0.025	0.048±0.008
L2	0.012±0.003	0.005±0.004	0.024±0.042	0.041±0.039

3.1 $ClNO_2$ production yields

Figure 3 shows $ClNO_2$ yields as a function of RH for the two samples with high chloride content (H1 and H2), and $\varphi(\mathrm{ClNO_2})$ were found to be quite high for the two samples. To be more specific, the mass fraction of chloride was 0.3870 for sample H1, and $\varphi(\mathrm{ClNO_2})$ were found to increase from 0.402±0.138 at 18% RH to 0.774±0.028 at 56% RH, and then slightly decreased to

0.697±0.311 when RH was further increased to 75%. For sample H2, the mass fraction of chloride (0.2145) was lower than sample H1, and $\varphi(ClNO_2)$ showed a small decrease (or remained relatively constant) when RH was increased from 18% to 56%, ranging from 0.474±0.026 to 0.560±0.046; further increase in RH to 75% resulted in small decrease in $\varphi(ClNO_2)$ to 0.378±0.069.

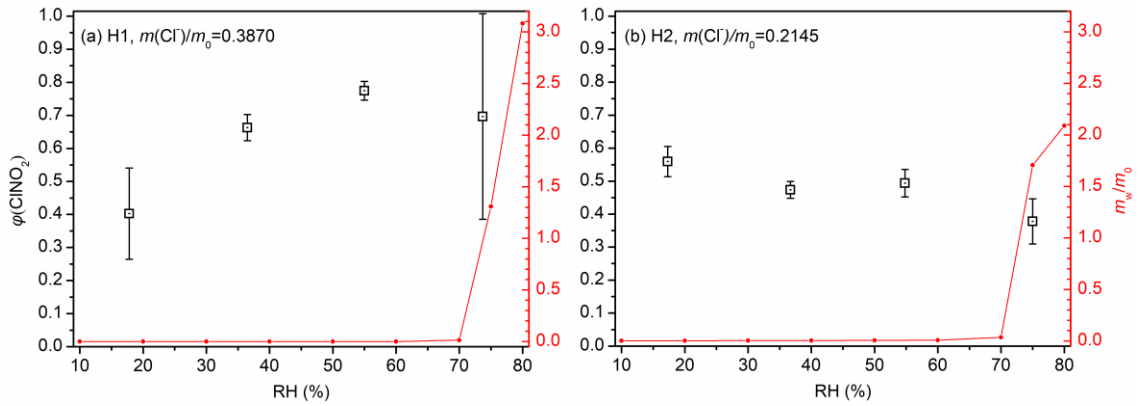

Figure 3. Measured $ClNO_2$ yields (black symbol) and m_w/m_0 (red line) as a function of RH for (a) H1 and (b) H2. The error bar represents standard deviation, and m_w/m_0 represents normalized mass of particulate water (normalized to the mass of dry particles), which was measured as the relative increase in particle mass at a given RH compared to <1% RH.

$ClNO_2$ yields are shown in Figure 4 as a function of RH for the two low chloride samples (L1 and L2), and their mass fractions of chloride were <0.01. As shown in Figure 4, $\varphi(ClNO_2)$ were found to be always <0.05 for the two samples, suggesting that heterogeneous production of $ClNO_2$ was very limited, despite substantial removal of N_2O_5 due to heterogeneous reaction (with an example shown in Figure 2c). The low $\varphi(ClNO_2)$ values for sample L1 and L2 could be attributed to their low chloride contents. In addition, $\varphi(ClNO_2)$ appeared to increase with RH for L1 and L2; however, since the uncertainties associated with $\varphi(ClNO_2)$ were rather large for these two samples, the dependence of $\varphi(ClNO_2)$ on RH should be treated in caution.

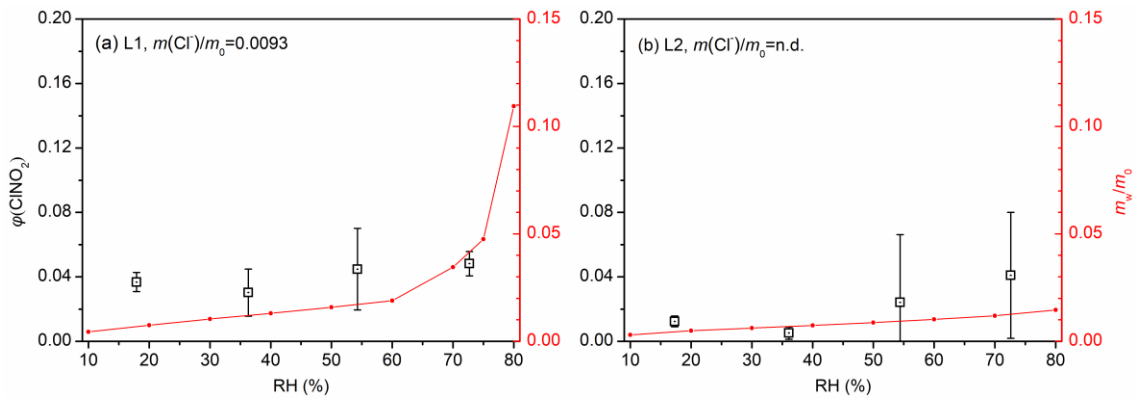

Figure 4. Measured $ClNO_2$ yields (black symbol) and m_w/m_0 (red line) as a function of RH for (a) L1 and (b) L2. The error bar represents standard deviation, and m_w/m_0 represents normalized mass of particulate water (normalized to the mass of dry particles), which was measured as the relative increase in particle mass at a given RH compared to <1% RH.

We also investigated $ClNO_2$ production from heterogeneous reaction of N_2O_5 with four samples with medium chloride contents (M1, M2, M3 and M4), and the results are displayed in Figure 5. Mass fractions of chloride were determined to be 0.0508 for M1, 0.034 for M2, 0.0229 for M3 and 0.0095 for M4, respectively. $ClNO_2$ yields were found to increase significantly with RH for M1 and M2; more specifically, $\varphi(ClNO_2)$ increased from 0.271±0.038 at 18% RH to 0.543±0.086 at 75% RH for sample M1, and increased from 0.166±0.018 at 18% RH to 0.418±0.0052 at 75% RH for sample M2. As shown in Figure 5, the dependence of $\varphi(ClNO_2)$ on RH for the other two medium chloride samples (M3 and M4) were rather different from M1 and M2. For sample M3, $\varphi(ClNO_2)$ first increased from 0.223±0.061 at 18% RH to 0.251±0.050 at 36% RH, and further increase in RH to 75% caused substantial reduction in $\varphi(ClNO_2)$. At last, no significant variation of $\varphi(ClNO_2)$ with RH (18-75%) was observed for sample M4.

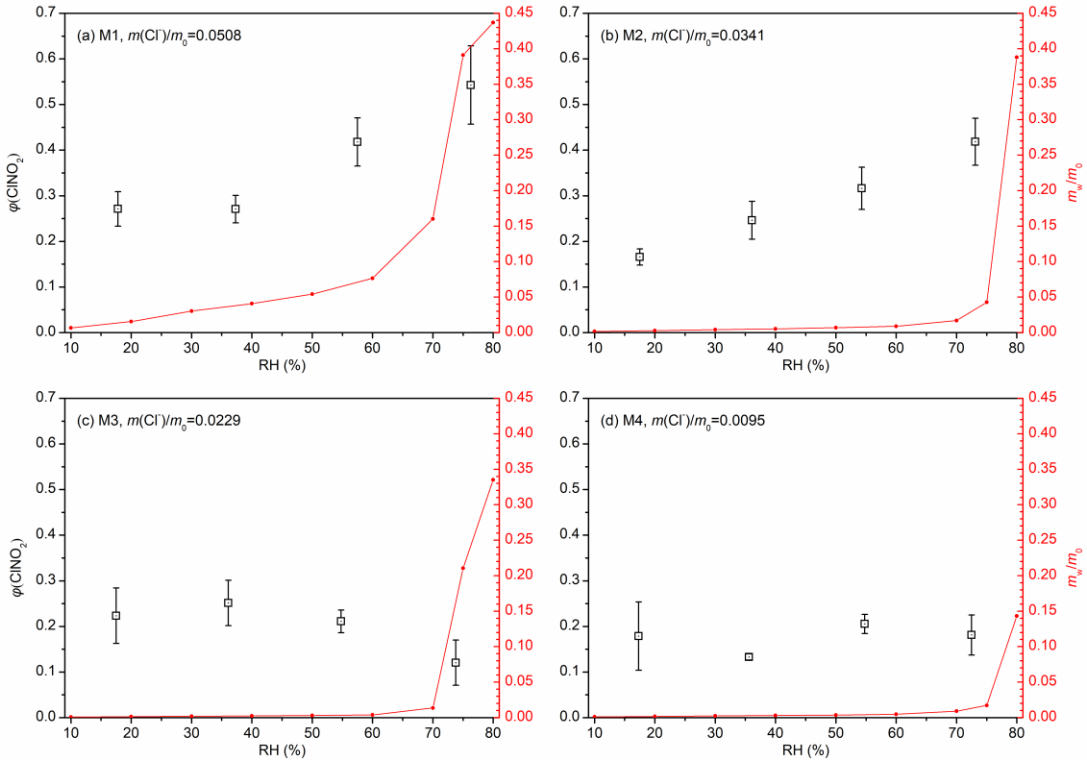

Figure 5. Measured $ClNO_2$ yields (black symbol) and m_w/m_0 (red line) as a function of RH for (a) M1, (b) M2, (c) M3, and (d) M4. The error bar represents standard deviation, and m_w/m_0 represents normalized mass of particulate water (normalized to the mass of dry particles), which was measured as the relative increase in particle mass at a given RH compared to <1% RH.

3.2 The effects of RH

The dependence of $\varphi(ClNO_2)$ on RH for the eight saline mineral samples we examined, as discussed in Section 3.1, exhibited two interesting features. First, when RH was as low as 18%, large $\varphi(ClNO_2)$ values (>0.2) were observed for four samples (H1, H2, M1 and M3). As the deliquescence RH of NaCl is ~75%, one may wonder where aqueous chloride, which is necessary for heterogeneous formation of $ClNO_2$, came from at 18% RH. As initially suggested by a previous study (Mitroo et al., 2019), the occurrence of aqueous chloride in saline mineral dust particles at low RH could be due to the presence of $CaCl_2$ and $MgCl_2$, which were amorphous under dry

conditions and could take up water at very low RH (Guo et al., 2019). Our previous study (Tang et al., 2019) measured water soluble ions contained by the eight saline mineral dust samples, and as shown in Figure S1, the amounts of water soluble Ca^{2+} in the four samples (H1, H2, M1 and M3) with larger $\varphi(ClNO_2)$ at 18% RH were significantly larger than those in the other four samples (M2, M4, L1 and L2). This observation further supported our deduction that the presence of $CaCl_2$ enabled efficient formation of $ClNO_2$ at low RH.

The second interesting feature is that as shown in Figures 3-5, $\varphi(ClNO_2)$ could increase, decrease or remain relatively constant with increase in RH from 18% to 75%. This feature can be understood given the complex mechanisms driving heterogeneous uptake of N_2O_5 onto saline mineral dust (Mitroo et al., 2019; Royer et al., 2021): at a given RH, N_2O_5 can react with aqueous water, aqueous chloride and insoluble minerals, and only its reaction with aqueous chloride would produce $ClNO_2$. The possible effects of RH on $\varphi(ClNO_2)$ are discussed below: 1) as RH increases, heterogeneous reactivity of N_2O_5 towards insoluble minerals can be enhanced, suppressed or remain largely unchanged (Tang et al., 2012; Tang et al., 2017); 2) increase in RH would lead to further hygroscopic growth and dilution of aqueous solutions, leading to decrease in $\varphi(ClNO_2)$ in this aspect; 3) the increase in particulate water with RH would cause more chloride to be dissolved into aqueous solutions, and in this aspect increase in RH would promote $ClNO_2$ formation. As a result, it is not surprised to observe different dependence of $\varphi(ClNO_2)$ on RH for different saline mineral dust samples.

3.3 Discussion

Figure 6 shows the dependence of $\varphi(ClNO_2)$ on mass fractions of chloride for the eight samples we examined at four different RH. These samples showed significant variation in

$\varphi(ClNO_2)$, ranging from <0.1 to >0.7, and $\varphi(ClNO_2)$ were largest for the two high chloride samples (H1 and H2), followed by median (M1, M2, M3 and M4) and low chloride samples (L1 and L2). Overall, a positive dependence of $\varphi(ClNO_2)$ on mass fractions of chloride was observed at each RH. Figure 6 also reveals that the measured $\varphi(ClNO_2)$ were very sensitive to mass fractions of chloride when the mass fractions of chloride were below 10%. However, as shown in Figure 6, higher chloride contents did not always mean larger $\varphi(ClNO_2)$, and similar observations were also reported by previous work (Mitroo et al., 2019; Royer et al., 2021). Furthermore, Figure 6 suggests that when mass fractions of chloride was <10%, the dependence of $\varphi(ClNO_2)$ on Cl contents was stronger at higher RH. This is because increase in RH would promote dissolution of chloride to aqueous water and thus enhance $ClNO_2$ formation.

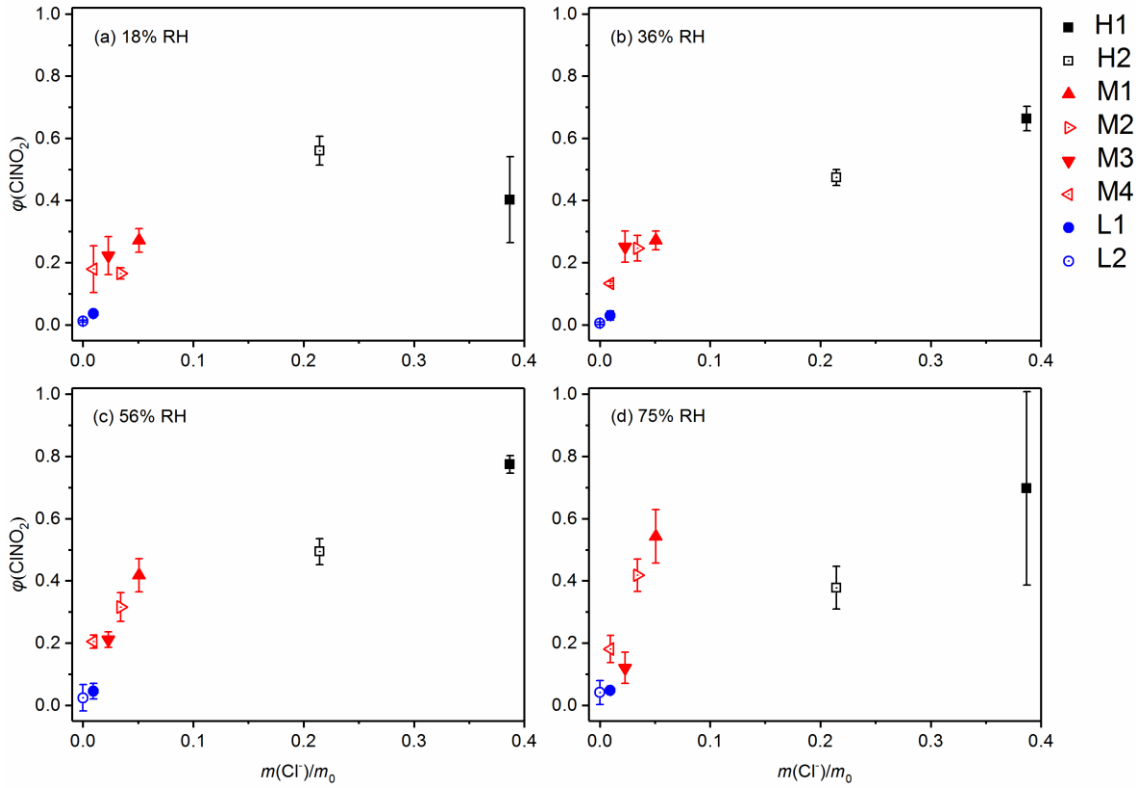

Figure 6. Dependence of $ClNO_2$ yields on mass fractions of chloride for the eight saline mineral dust samples at a given RH: a) 18% RH; b) 36% RH; c) 56% RH; d) 75% RH.

Two parameterizations have been widely used to predict the dependence of $\varphi(ClNO_2)$ on chemical compositions and water contents of aqueous aerosol particles (Bertram and Thornton, 2009; Yu et al., 2020). Based on laboratory results, Bertram and Thornton (2009) suggested that $ClNO_2$ yields can be calculated using Eq. (2):

$$\varphi(ClNO_2) = \left(1 + \frac{k(H_2O)\cdot[H_2O_{(aq)}]}{k(Cl^-)\cdot[Cl^-]}\right)^{-1} \quad (2)$$

where $[H_2O_{(aq)}]/[Cl^-]$ is the ratio of molar concentration of H_2O to that of Cl^- in aqueous particles, and the value of $k(H_2O)/k(Cl^-)$ was suggested to be 1/(483±175) (Bertram and Thornton, 2009). Very recently, Yu et al. (2020) examined uptake coefficients of N_2O_5 onto ambient aerosol particles at four different sites in China, and suggested that using a value of 1/(105±37) for $k(H_2O)/k(Cl^-)$ would lead to better agreement between measured and predicted uptake coefficients of N_2O_5 (Yu et al., 2020).

The two parameterizations were used in our work to calculate $\varphi(ClNO_2)$ at 75% RH for the eight saline mineral dust samples we examined. $[H_2O_{(aq)}]/[Cl^-]$ was calculated from the measured mass growth factors at 75% RH and the mass fractions of chloride, assuming that all the chloride contained by saline mineral dust samples was dissolved into aqueous solutions at 75% RH. The comparison between measured and calculated $\varphi(ClNO_2)$ is displayed in Figure 7, suggesting that both parameterizations significantly overestimated the measured $\varphi(ClNO_2)$ for all the eight saline mineral dust samples we investigated. A previous study (Mitroo et al., 2019) investigated $\varphi(ClNO_2)$ for heterogeneous uptake of N_2O_5 onto saline mineral dust samples collected in southwestern USA, and similarly they found that the measured $\varphi(ClNO_2)$ were significantly smaller than those predicted using the parameterization proposed by Bertram and Thornton (2009).

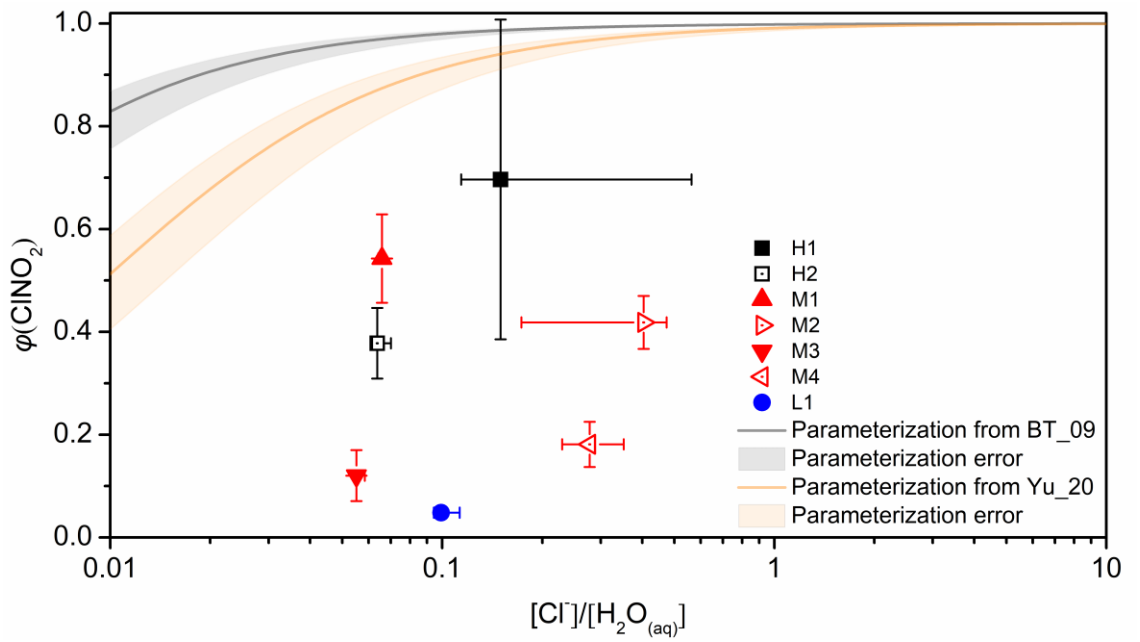

352

353 **Figure 7.** Measured and calculated of $\varphi(ClNO_2)$ at 75±2% RH as a function of $[Cl^-]/[H_2O_{(aq)}]$.
354 Black and orange curves represent $\varphi(ClNO_2)$ calculated using the BT_09 parameterization
355 (Bertram and Thornton, 2009) and the Yu_20 parameterization (Yu et al., 2020), and the associated
356 errors are represented by the corresponding shadows.

357

358 The observed discrepancies between measured and predicted $\varphi(ClNO_2)$ can be caused by
359 several reasons. First, even at ~75% RH (the highest RH at which our experiments were conducted),
360 chloride contained in saline mineral dust may not be fully dissolved, and therefore our calculation
361 may overestimate $[Cl^-]/[H_2O_{(aq)}]$ and thus also overestimate $\varphi(ClNO_2)$. This effect should not be
362 large as significant water uptake was observed at ~75% RH for saline mineral dust sample we
363 examined (Figures 3-5). Second, perhaps more importantly, saline mineral dust samples contain
364 substantial amounts of insoluble minerals, and some of these minerals, such as clays, are very
365 reactive towards N_2O_5 (Tang et al., 2017), and only nitrate but no $ClNO_2$ was formed (Seisel et al.,
366 2005; Karagulian et al., 2006; Tang et al., 2012). However, the two parameterizations did not take
367 into account heterogeneous reaction of N_2O_5 with insoluble minerals, and as a result would

inevitably overestimate $\varphi(ClNO_2)$. At last, our calculations assumed internal mixing, but inter- and intra-particle heterogeneity of saline mineral dust particles could also contribute to the observed gap between measured and calculated $\varphi(ClNO_2)$. For example, a wintertime field campaign at Ann Arbor (Michigan, USA) (McNamara et al., 2020) showed that due to nonhomogeneous chloride distribution across road salt aerosol particles, observed $\varphi(ClNO_2)$ were significantly smaller than predicted values. The comparison between measured and predicted $\varphi(ClNO_2)$ suggested that while heterogeneous uptake of N_2O_5 onto saline mineral dust could be an important source of inland $ClNO_2$, underlying mechanisms which affect heterogeneous production of $ClNO_2$ from saline mineral dust have not been well elucidated.

4 Atmospheric implications

We consider $ClNO_2$ formation in heterogeneous uptake of N_2O_5 onto dust aerosol in GEOS-Chem to explore its atmospheric implications. Since Cl^- concentration in mineral dust is not well known and currently we are not able to parameterize $\varphi(ClNO_2)$ for mineral dust (as discussed in Section 3.3), we use a fixed $\varphi(ClNO_2)$ value of 0.1 in our simulation. This value, which is at the low end of our measured range of $\varphi(ClNO_2)$ (<0.05 to ~0.77), is higher than those determined in our work for low chloride samples but lower than those for medium chloride samples. The purpose of our modeling work, is to preliminarily assess whether N_2O_5 uptake onto saline dust may have important effects on tropospheric chemistry as a potential source of $ClNO_2$. We focus on simulations on 2-7 May 2017, during which a large dust event took place in East Asia. It caused high concentrations of dust aerosols with maximum hourly concentration higher than 1000 $\mu g/m^3$ over a wide area in China (Zhang et al., 2018), which are also well captured by our simulations (Figure S2).

Figure 8 shows the weekly mean values of the nighttime maximum surface $ClNO_2$ mixing ratios and the contribution of heterogeneous reaction of N_2O_5 with dust aerosol to $ClNO_2$ over 2-7 May 2017. The impact of N_2O_5 uptake onto dust aerosol is calculated as the difference between the standard case in which $\varphi(ClNO_2)$ is assumed to be 0 for N_2O_5 uptake onto dust aerosol and the case in which $\varphi(ClNO_2)$ is assumed to be 0.1. Due to large diurnal variations and near-zero mixing ratios of $ClNO_2$ in the daytime, we use the mean nighttime maximum value for $ClNO_2$, following previous standard practice (Wang et al., 2019). The largest impact on $ClNO_2$ is found in Central China, where weekly mean nighttime maximum surface $ClNO_2$ mixing ratios are increased by 85 pptv, due to heavy impact of dust aerosol transported from the north and high NO_x emissions in this region. Even larger effects (up to 240 pptv increase in $ClNO_2$) can be found on some individual days, as shown in Figures S3 and S4. These results suggest that N_2O_5 uptake onto dust could be an important source for tropospheric $ClNO_2$ over Central and Northeast China, where $ClNO_2$ formation is conventionally believed to be limited due to relatively low aerosol chloride levels from sea salts and anthropogenic sources.

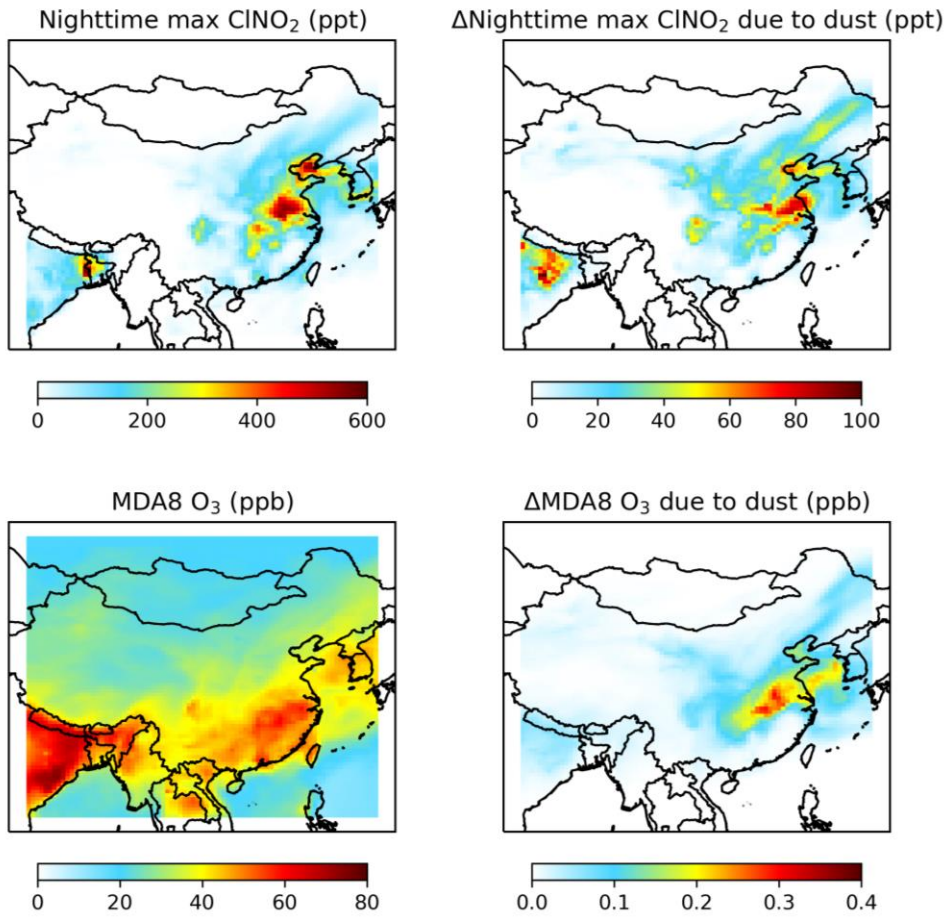

405

406 **Figure 8.** Modeled weekly mean mixing ratios of nighttime maximum $ClNO_2$ (upper panels) and
407 maximum daily 8-h average (MDA8) ozone (bottom panels) in surface air over China during 2-7
408 May 2017. The left panels show simulated mixing ratios in our standard case in which $\varphi(ClNO_2)$
409 is assumed to be 0 for N_2O_5 uptake onto dust aerosol. The right panels show impacts of $ClNO_2$
410 formation due to N_2O_5 uptake onto dust, calculated as the difference between the standard case
411 and the case in which $\varphi(ClNO_2)$ is assumed to be 0.1 for N_2O_5 uptake onto dust.

412

413 Figure 8 also shows the effect of $ClNO_2$ formation due to heterogeneous reaction of N_2O_5
414 with dust aerosol on the daily maximum 8-h average (MDA8) ozone mixing ratios in the surface
415 air over China during the same period. MDA8 ozone mixing ratios are increased by up to 0.32

ppbv after considering mineral dust as an additional source of $ClNO_2$. Our simulation assumes a low value of $\varphi(ClNO_2)$ in our measured range (<0.05 to ~0.77), and is conducted in summer when $ClNO_2$ is more difficult to be accumulated due to short night (compared to winter and spring with long nights). We expect that its impacts on $ClNO_2$ and ozone could be larger for dust events in winter and spring.

5 Conclusions

It has been widely recognized that nitryl chloride ($ClNO_2$), produced by heterogeneous reaction of N_2O_5 with chloride-containing aerosols, could significantly affect atmospheric oxidation capacity. However, heterogeneous formation of tropospheric $ClNO_2$ in inland regions in China has not been well elucidated. In this work, we investigated $ClNO_2$ formation in heterogeneous reaction of N_2O_5 with eight saline mineral dust samples collected from different regions in China as a function of RH (18-75%). Significant production of $ClNO_2$ was observed for some of the saline mineral dust samples examined, and $ClNO_2$ yields, $\varphi(ClNO_2)$, were determined to span from <0.05 to 0.77, depending on chemical compositions of saline mineral dust samples and RH. In general a positive dependence of $\varphi(ClNO_2)$ on mass fractions of particulate chloride was observed at each RH, but higher particulate chloride content did not always result in higher $\varphi(ClNO_2)$. On the other hand, increase in RH could increase, reduce or have no significant impacts on $\varphi(ClNO_2)$, revealing the complex mechanisms which drive heterogeneous uptake of N_2O_5 onto saline mineral dust.

Two widely-used parameterizations (Bertram and Thornton, 2009; Yu et al., 2020) were used to estimate $\varphi(ClNO_2)$ at 75% RH for the eight saline mineral dust samples we investigated. Both parameterizations were found to significantly overestimate the measured $\varphi(ClNO_2)$, and we

suggested that the discrepancies between measured and predicted $\varphi(ClNO_2)$ could be due to incomplete dissolution of particulate chloride, heterogeneous reaction of N_2O_5 with insoluble minerals, and/or inter- and intra-particle heterogeneity of saline mineral dust particles.

Assuming a $\varphi(ClNO_2)$ value of 0.1 for heterogeneous reaction of N_2O_5 with mineral dust, we use GEOS-Chem to assess the impact of this reaction on tropospheric $ClNO_2$ and O_3 in China during a severe dust event which occurred during 2-7 May 2017. It is found that after taking into account $ClNO_2$ production due to N_2O_5 uptake onto mineral dust aerosol, weekly mean nighttime maximum $ClNO_2$ mixing ratios could be increased by up to 85 pptv during this period and the daily maximum 8-h average O_3 mixing ratios were increased by up to 0.32 ppbv.

In summary, our work shows that heterogeneous reaction of N_2O_5 with saline mineral dust can be an important source for tropospheric $ClNO_2$ in inland China. This reaction may also be important for tropospheric $ClNO_2$ production in many other regions over the world, as the occurrence of saline mineral dust aerosols has been reported in various locations, such as Iran (Gholampour et al., 2015), United States (Blank et al., 1999; Pratt et al., 2010; Jordan et al., 2015; Frie et al., 2017), and Argentina (Bucher and Stein, 2016). Currently our limited knowledge precludes quantitative prediction of heterogeneous $ClNO_2$ production from saline mineral dust, and further investigation is thus warranted.

Appendix. N_2O_5 and $ClNO_2$ calibration

To calibrate CIMS measurements of N_2O_5, a mixed flow containing N_2O_5, which was produced via O_3 oxidation of NO_2, was sampled into the CIMS instrument, and N_2O_5 was quantified using the normalized intensities of $I(N_2O_5)^-$ clusters, $f(N_2O_5)$, defined as the ratio of signal intensity (cps) of $I(N_2O_5)^-$ to that of the total reagent ions, i.e. I^- and $I(H_2O)^-$. N_2O_5

concentrations in the mixed flow were quantified using cavity-enhanced absorption spectroscopy (CEAS) (Wang et al., 2017a), with a detection limit of 2.7 pptv in 5 s and an uncertainty of ~25%. RH of the mixed flow was varied during the calibration in order to determine the CIMS sensistivity for N_2O_5 at different RH, and the results are displayed in Figure A1. The sensitivity for N_2O_5 first increased with RH, reaching the maximum value at ~40% RH, and then decreased with further increase in RH.

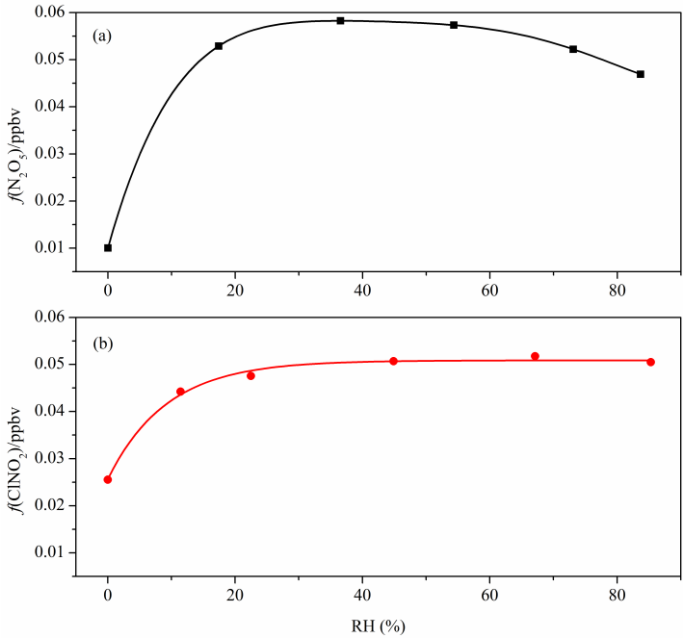

Figure A1. CIMS sensitivities as a function of RH for (a) N_2O_5 and (b) $ClNO_2$.

To calibrate CIMS measurements of $ClNO_2$, a nitrogen flow (6 mL/min) containing 10 ppmv Cl_2 was passed over a slurry containing $NaNO_2$ and NaCl to produce $ClNO_2$ (Thaler et al., 2011), and NaCl was included in the slurry in order to minimize the formation of NO_2 as a byproduct. The mixed flow containing $ClNO_2$ was then conditioned to a given RH and sampled into the CIMS instrument; similar to N_2O_5, $ClNO_2$ was quantified using the normalized intensities of $I(ClNO_2)^-$ clusters, $f(ClNO_2)$, defined as the ratio of signal intensity (cps) of $I(ClNO_2)^-$ to that of the total

reagent ions. To quantify $ClNO_2$, the mixed flow was delivered directly into a cavity attenuated phase shift spectroscopy instrument (CAPS, Model N500, Teledyne API) to measure background NO_2 concentrations; after that, the mixed flow was delivered through a thermal dissociation model at 365 ^oC to fully decompose $ClNO_2$ to NO_2, and the total NO_2 concentrations were then determined using CAPS. The differences in the measured NO_2 concentrations with and without thermal dissociation was equal to $ClNO_2$ concentrations. The CAPS instrument had a detection limit of 0.2 ppbv in 1 min for NO_2 and an uncertainty of ~10%. As shown in Figure A1, the sensitivity for $ClNO_2$ increased with RH up to 40%, and showed little variation with further increase in RH.

Data availability

Data used in this paper can be found in the main text or supplement. GEOS-Chem model is available at GEOS-Chem repository (http://www.geos-chem.org).

Competing interests

The authors declare that they have no conflict of interest.

Author contribution

Haichao Wang: investigation, formal analysis, writing-original draft, writing – review & editing; **Chao Peng:** investigation, formal analysis, writing-original draft, writing – review & editing; **Xuan Wang:** investigation, formal analysis, writing-original draft, writing – review & editing; **Shengrong Lou:** resources; **Keding Lu:** resources, supervision; **Guicheng Gan:** investigation; **Xiaohong Jia:** investigation; **Xiaorui Chen:** investigation; **Jun Chen:** supervision; **Hongli Wang:** resources; **Shaojia Fan:** resources; **Xinming Wang:** resources; **Mingjin Tang:** conceptualization, formal analysis, resources, supervision, writing-original draft, writing-review & editing.

Financial support

This work was funded by National Natural Science Foundation of China (41907185, 42022050 and 91744204), Ministry of Science and Technology of China (2018YFC0213901), Guangdong Basic and Applied Basic Research Fund Committee (2020B1515130003), National State Environmental Protection Key Laboratory of Formation and Prevention of Urban Air Pollution Complex (CX2020080094 and CX2020080578), Guangdong Foundation for Program of Science and Technology Research (2019B121205006 and 2020B1212060053), Guangdong Science and Technology Department (2017GC010501) and CAS Pioneer Hundred Talents program.

Reference

Abuduwailli, J., Gabchenko, M. V., and Xu, J.: Eolian transport of salts - A case study in the area of Lake Ebinur (Xinjiang, Northwest China), Journal of Arid Environments, 72, 1843-1852, 2008.

Ahern, A., Goldberger, L., Jahl, L., Thornton, J., and Sullivan, R. C.: Production of N2O5 and ClNO2 through nocturnal processing of biomass-burning aerosol, Environmental science & technology, 52, 550-559, 2017.

Atkinson, R., and Arey, J.: Atmospheric degradation of volatile organic compounds, Chemical Reviews, 103, 4605-4638, 2003.

Atkinson, R., Baulch, D. L., Cox, R. A., Crowley, J. N., Hampson, R. F., Hynes, R. G., Jenkin, M. E., Rossi, M. J., and Troe, J.: Evaluated kinetic and photochemical data for atmospheric chemistry: Volume II - gas phase reactions of organic species, Atmospheric Chemistry and Physics, 6, 3625-4055, 2006.

Bannan, T. J., Booth, A. M., Bacak, A., Muller, J. B. A., Leather, K. E., Le Breton, M., Jones, B., Young, D., Coe, H., Allan, J., Visser, S., Slowik, J. G., Furger, M., Prevot, A. S. H., Lee, J., Dunmore, R. E., Hopkins, J. R., Hamilton, J. F., Lewis, A. C., Whalley, L. K., Sharp, T., Stone, D., Heard, D. E., Fleming, Z. L., Leigh, R., Shallcross, D. E., and Percival, C. J.: The first UK measurements of nitryl chloride using a chemical ionization mass spectrometer in central London in the summer of 2012, and an investigation of the role of Cl atom oxidation, Journal of Geophysical Research-Atmospheres, 120, 5638-5657, 2015.

Bannan, T. J., Khan, M. A. H., Le Breton, M., Priestley, M., Worrall, S. D., Bacak, A., Marsden, N. A., Lowe, D., Pitt, J., Shallcross, D. E., and Percival, C. J.: A Large Source of Atomic Chlorine From ClNO2 Photolysis at a UK Landfill Site, Geophysical Research Letters, 46, 8508-8516, 2019.

Bertram, T. H., and Thornton, J. A.: Toward a general parameterization of N2O5 reactivity on aqueous particles: the competing effects of particle liquid water, nitrate and chloride, Atmospheric Chemistry And Physics, 9, 8351-8363, 2009.

Blank, R. R., Young, J. A., and Allen, F. L.: Aeolian dust in a saline playa environment, Nevada, USA, Journal of Arid Environments, 41, 365-381, 1999.
Bucher, E. H., and Stein, A. F.: Large Salt Dust Storms Follow a 30-Year Rainfall Cycle in the Mar Chiquita Lake (Cordoba, Argentina), Plos One, 11, 2016.
Crowley, J. N., Ammann, M., Cox, R. A., Hynes, R. G., Jenkin, M. E., Mellouki, A., Rossi, M. J., Troe, J., and Wallington, T. J.: Evaluated kinetic and photochemical data for atmospheric chemistry: Volume V – heterogeneous reactions on solid substrates, Atmos. Chem. Phys., 10, 9059-9223, 2010.
Eger, P. G., Friedrich, N., Schuladen, J., Shenolikar, J., Fischer, H., Tadic, I., Harder, H., Martinez, M., Rohloff, R., Tauer, S., Drewnick, F., Fachinger, F., Brooks, J., Darbyshire, E., Sciare, J., Pikridas, M., Lelieveld, J., and Crowley, J. N.: Shipborne measurements of ClNO2 in the Mediterranean Sea and around the Arabian Peninsula during summer, Atmospheric Chemistry and Physics, 19, 12121-12140, 2019.
Faxon, C. B., Bean, J. K., and Hildebrandt Ruiz, L.: Inland Concentrations of Cl-2 and ClNO2 in Southeast Texas Suggest Chlorine Chemistry Significantly Contributes to Atmospheric Reactivity, Atmosphere, 6, 1487-1506, 2015.
Fountoukis, C., and Nenes, A.: ISORROPIA II: a computationally efficient thermodynamic equilibrium model for K+-Ca2+-Mg2+-Nh(4)(+)-Na+-SO42--NO3--Cl--H2O aerosols, Atmospheric Chemistry and Physics, 7, 4639-4659, 2007.
Frie, A. L., Dingle, J. H., Ying, S. C., and Bahreini, R.: The Effect of a Receding Saline Lake (The Salton Sea) on Airborne Particulate Matter Composition, Environmental Science & Technology, 51, 8283-8292, 2017.
Fu, X., Wang, T., Wang, S., Zhang, L., Cai, S., Xing, J., and Hao, J.: Anthropogenic Emissions of Hydrogen Chloride and Fine Particulate Chloride in China, Environ Sci Technol, 52, 1644-1654, 2018.
Gaston, C. J., Pratt, K. A., Suski, K. J., May, N. W., Gill, T. E., and Prather, K. A.: Laboratory Studies of the Cloud Droplet Activation Properties and Corresponding Chemistry of Saline Playa Dust, Environmental Science & Technology, 51, 1348-1356, 2017.
Gaston, C. J.: Re-examining Dust Chemical Aging and Its Impacts on Earth's Climate, Accounts of Chemical Research, 53, 1005-1013, 2020.
Gholampour, A., Nabizadeh, R., Hassanvand, M. S., Taghipour, H., Nazmara, S., and Mahvi, A. H.: Characterization of saline dust emission resulted from Urmia Lake drying, Journal of Environmental Health Science and Engineering, 13, 2015.
Gillette, D., Stensland, G., Williams, A., Barnard, W., Gatz, D., Sinclair, P., and Johnson, T.: Emissions of alkaline elements calcium, magnesium, potassium, and sodium from open sources in the contiguous United States, Global Biogeochemical Cycles, 6, 437-457, 1992.
Gu, W., Li, Y., Zhu, J., Jia, X., Lin, Q., Zhang, G., Ding, X., Song, W., Bi, X., Wang, X., and Tang, M.: Investigation of water adsorption and hygroscopicity of atmospherically relevant particles using a commercial vapor sorption analyzer, Atmospheric Measurement Techniques, 10, 3821-3832, 2017.
Guo, L., Gu, W., Peng, C., Wang, W., Li, Y. J., Zong, T., Tang, Y., Wu, Z., Lin, Q., Ge, M., Zhang, G., Hu, M., Bi, X., Wang, X., and Tang, M.: A comprehensive study of hygroscopic properties of calcium- and magnesium-containing salts: implication for hygroscopicity of mineral dust and sea salt aerosols, Atmospheric Chemistry and Physics, 19, 2115-2133, 2019.
Jia, X., Gu, W., Peng, C., Li, R., Chen, L., Wang, H., Wang, H., Wang, X., and Tang, M.: Heterogeneous reaction of CaCO3 with NO2 at different relative humidities: Kinetics,

mechanisms, and impacts on aerosol hygroscopicity, Journal of Geophysical Research-Atmospheres, 126, e2021JD034826, 2021.
Jordan, C. E., Pszenny, A. A. P., Keene, W. C., Cooper, O. R., Deegan, B., Maben, J., Routhier, M., Sander, R., and Young, A. H.: Origins of aerosol chlorine during winter over north central Colorado, USA, Journal of Geophysical Research-Atmospheres, 120, 678-694, 2015.
Karagulian, F., Santschi, C., and Rossi, M. J.: The heterogeneous chemical kinetics of N2O5 on CaCO3 and other atmospheric mineral dust surrogates, Atmospheric Chemistry and Physics, 6, 1373-1388, 2006.
Kercher, J. P., Riedel, T. P., and Thornton, J. A.: Chlorine activation by N2O5: simultaneous, in situ detection of ClNO2 and N2O5 by chemical ionization mass spectrometry, Atmospheric Measurement Techniques, 2, 193-204, 2009.
Le Breton, M., Hallquist, A. M., Pathak, R. K., Simpson, D., Wang, Y., Johansson, J., Zheng, J., Yang, Y., Shang, D., Wang, H., Liu, Q., Chan, C., Wang, T., Bannan, T. J., Priestley, M., Percival, C. J., Shallcross, D. E., Lu, K., Guo, S., Hu, M., and Hallquist, M.: Chlorine oxidation of VOCs at a semi-rural site in Beijing: significant chlorine liberation from ClNO2 and subsequent gas- and particle-phase Cl-VOC production, Atmospheric Chemistry and Physics, 18, 13013-13030, 2018.
Li, R., Jia, X., Wang, F., Ren, Y., Wang, X., Zhang, H., Li, G., Wang, X., and Tang, M.: Heterogeneous reaction of NO2 with hematite, goethite and magnetite: Implications for nitrate formation and iron solubility enhancement, Chemosphere, 242, 125273-125273, 2020.
Lu, K., Guo, S., Tan, Z., Wang, H., Shang, D., Liu, Y., Li, X., Wu, Z., Hu, M., and Zhang, Y.: Exploring atmospheric free-radical chemistry in China: the self-cleansing capacity and the formation of secondary air pollution, National Science Review, 6, 579-594, 2019.
McDuffie, E. E., Fibiger, D. L., Dube, W. P., Hilfiker, F. L., Lee, B. H., Jaegle, L., Guo, H., Weber, R. J., Reeves, J. M., Weinheimer, A. J., Schroder, J. C., Campuzano-Jost, P., Jimenez, J. L., Dibb, J. E., Veres, P., Ebben, C., Sparks, T. L., Wooldridge, P. J., Cohen, R. C., Campos, T., Hall, S. R., Ullmann, K., Roberts, J. M., Thornton, J. A., and Brown, S. S.: ClNO2 Yields From Aircraft Measurements During the 2015 WINTER Campaign and Critical Evaluation of the Current Parameterization, Journal of Geophysical Research-Atmospheres, 123, 12994-13015, 2018a.
McDuffie, E. E., Fibiger, D. L., Dube, W. P., Lopez-Hilfiker, F., Lee, B. H., Thornton, J. A., Shah, V., Jaegle, L., Guo, H., Weber, R. J., Reeves, J. M., Weinheimer, A. J., Schroder, J. C., Campuzano-Jost, P., Jimenez, J. L., Dibb, J. E., Veres, P., Ebben, C., Sparks, T. L., Wooldridge, P. J., Cohen, R. C., Hornbrook, R. S., Apel, E. C., Campos, T., Hall, S. R., Ullmann, K., and Brown, S. S.: Heterogeneous N2O5 Uptake During Winter: Aircraft Measurements During the 2015 WINTER Campaign and Critical Evaluation of Current Parameterizations, Journal of Geophysical Research-Atmospheres, 123, 4345-4372, 2018b.
McNamara, S. M., Kolesar, K. R., Wang, S., Kirpes, R. M., May, N. W., Gunsch, M. J., Cook, R. D., Fuentes, J. D., Hornbrook, R. S., Apel, E. C., China, S., Laskin, A., and Pratt, K. A.: Observation of Road Salt Aerosol Driving Inland Wintertime Atmospheric Chlorine Chemistry, Acs Central Science, 6, 684-694, 2020.
Mielke, L. H., Furgeson, A., and Osthoff, H. D.: Observation of ClNO2 in a Mid-Continental Urban Environment, Environmental Science & Technology, 45, 8889-8896, 2011.
Mielke, L. H., Furgeson, A., Odame-Ankrah, C. A., and Osthoff, H. D.: Ubiquity of ClNO2 in the urban boundary layer of Calgary, Alberta, Canada, Canadian Journal of Chemistry, 94, 414-423, 2016.

628 Mitroo, D., Gill, T. E., Haas, S., Pratt, K. A., and Gaston, C. J.: ClNO2 Production from N2O5
629 Uptake on Saline Playa Dusts: New Insights into Potential Inland Sources of ClNO2, Environ
630 Sci Technol, 53, 7442-7452, 2019.
631 Osthoff, H. D., Roberts, J. M., Ravishankara, A. R., Williams, E. J., Lerner, B. M., Sommariva,
632 R., Bates, T. S., Coffman, D., Quinn, P. K., Dibb, J. E., Stark, H., Burkholder, J. B., Talukdar,
633 R. K., Meagher, J., Fehsenfeld, F. C., and Brown, S. S.: High levels of nitryl chloride in the
634 polluted subtropical marine boundary layer, Nature Geoscience, 1, 324-328, 2008.
635 Osthoff, H. D., Odame-Ankrah, C. A., Taha, Y. M., Tokarek, T. W., Schiller, C. L., Haga, D.,
636 Jones, K., and Vingarzan, R.: Low levels of nitryl chloride at ground level: nocturnal nitrogen
637 oxides in the Lower Fraser Valley of British Columbia, Atmospheric Chemistry and Physics,
638 18, 6293-6315, 2018.
639 Phillips, G. J., Tang, M. J., Thieser, J., Brickwedde, B., Schuster, G., Bohn, B., Lelieveld, J., and
640 Crowley, J. N.: Significant concentrations of nitryl chloride observed in rural continental Europe
641 associated with the influence of sea salt chloride and anthropogenic emissions, Geophysical
642 Research Letters, 39, 2012.
643 Pratt, K. A., Twohy, C. H., Murphy, S. M., Moffet, R. C., Heymsfield, A. J., Gaston, C. J., DeMott,
644 P. J., Field, P. R., Henn, T. R., Rogers, D. C., Gilles, M. K., Seinfeld, J. H., and Prather, K. A.:
645 Observation of playa salts as nuclei in orographic wave clouds, Journal of Geophysical
646 Research-Atmospheres, 115, 2010.
647 Ridley, D. A., Heald, C. L., Pierce, J. R., and Evans, M. J.: Toward resolution-independent dust
648 emissions in global models: Impacts on the seasonal and spatial distribution of dust,
649 Geophysical Research Letters, 40, 2873-2877, 2013.
650 Riedel, T. P., Bertram, T. H., Crisp, T. A., Williams, E. J., Lerner, B. M., Vlasenko, A., Li, S.-M.,
651 Gilman, J., de Gouw, J., Bon, D. M., Wagner, N. L., Brown, S. S., and Thornton, J. A.: Nitryl
652 Chloride and Molecular Chlorine in the Coastal Marine Boundary Layer, Environmental
653 Science & Technology, 46, 10463-10470, 2012.
654 Riedel, T. P., Wagner, N. L., Dube, W. P., Middlebrook, A. M., Young, C. J., Ozturk, F., Bahreini,
655 R., VandenBoer, T. C., Wolfe, D. E., Williams, E. J., Roberts, J. M., Brown, S. S., and Thornton,
656 J. A.: Chlorine activation within urban or power plant plumes: Vertically resolved ClNO2 and
657 Cl-2 measurements from a tall tower in a polluted continental setting, Journal of Geophysical
658 Research-Atmospheres, 118, 8702-8715, 2013.
659 Riedel, T. P., Wolfe, G. M., Danas, K. T., Gilman, J. B., Kuster, W. C., Bon, D. M., Vlasenko, A.,
660 Li, S. M., Williams, E. J., Lerner, B. M., Veres, P. R., Roberts, J. M., Holloway, J. S., Lefer, B.,
661 Brown, S. S., and Thornton, J. A.: An MCM modeling study of nitryl chloride (ClNO2) impacts
662 on oxidation, ozone production and nitrogen oxide partitioning in polluted continental outflow,
663 Atmospheric Chemistry and Physics, 14, 3789-3800, 2014.
664 Royer, H. M., Mitroo, D., Hayes, S. M., Haas, S. M., Pratt, K. A., Blackwelder, P. L., Gill, T. E.,
665 and Gaston, C. J.: The Role of Hydrates, Competing Chemical Constituents, and Surface
666 Composition on ClNO2 Formation, Environ Sci Technol, 2021.
667 Ryder, O. S., Ault, A. P., Cahill, J. F., Guasco, T. L., Riedel, T. P., Cuadra-Rodriguez, L. A.,
668 Gaston, C. J., Fitzgerald, E., Lee, C., Prather, K. A., and Bertram, T. H.: On the Role of Particle
669 Inorganic Mixing State in the Reactive Uptake of N2O5 to Ambient Aerosol Particles,
670 Environmental Science & Technology, 48, 1618-1627, 2014.
671 Saiz-Lopez, A., and von Glasow, R.: Reactive halogen chemistry in the troposphere, Chemical
672 Society Reviews, 41, 6448-6472, 2012.

673 Sarwar, G., Simon, H., Xing, J., and Mathur, R.: Importance of tropospheric ClNO2 chemistry
674 across the Northern Hemisphere, Geophysical Research Letters, 41, 4050-4058, 2014.
675 Seisel, S., Borensen, C., Vogt, R., and Zellner, R.: Kinetics and mechanism of the uptake of N2O5
676 on mineral dust at 298 K, Atmospheric Chemistry and Physics, 5, 3423-3432, 2005.
677 Simon, H., Kimura, Y., McGaughey, G., Allen, D. T., Brown, S. S., Osthoff, H. D., Roberts, J. M.,
678 Byun, D., and Lee, D.: Modeling the impact of ClNO2 on ozone formation in the Houston area,
679 Journal of Geophysical Research-Atmospheres, 114, 2009.
680 Simpson, W. R., Brown, S. S., Saiz-Lopez, A., Thornton, J. A., and von Glasow, R.: Tropospheric
681 Halogen Chemistry: Sources, Cycling, and Impacts, Chemical Reviews, 115, 4035-4062, 2015.
682 Tang, M., Huang, X., Lu, K., Ge, M., Li, Y., Cheng, P., Zhu, T., Ding, A., Zhang, Y., Gligorovski,
683 S., Song, W., Ding, X., Bi, X., and Wang, X.: Heterogeneous reactions of mineral dust aerosol:
684 implications for tropospheric oxidation capacity, Atmospheric Chemistry and Physics, 17,
685 11727-11777, 2017.
686 Tang, M., Zhang, H., Gu, W., Gao, J., Jian, X., Shi, G., Zhu, B., Xie, L., Guo, L., and Gao, X.:
687 Hygroscopic properties of saline mineral dust from different regions in China: geographical
688 variations, compositional dependence and atmospheric implications, Journal of Geophysical
689 Research: Atmospheres, 124, 10844-10857, 2019.
690 Tang, M. J., Thieser, J., Schuster, G., and Crowley, J. N.: Kinetics and mechanism of the
691 heterogeneous reaction of N2O5 with mineral dust particles, Physical Chemistry Chemical
692 Physics, 14, 8551-8561, 2012.
693 Thaler, R. D., Mielke, L. H., and Osthoff, H. D.: Quantification of Nitryl Chloride at Part Per
694 Trillion Mixing Ratios by Thermal Dissociation Cavity Ring-Down Spectroscopy, Analytical
695 Chemistry, 83, 2761-2766, 2011.
696 Tham, Y. J., Yan, C., Xue, L., Zha, Q., Wang, X., and Wang, T.: Presence of high nitryl chloride
697 in Asian coastal environment and its impact on atmospheric photochemistry, Chinese Science
698 Bulletin, 59, 356-359, 2014.
699 Tham, Y. J., Wang, Z., Li, Q., Yun, H., Wang, W., Wang, X., Xue, L., Lu, K., Ma, N., Bohn, B.,
700 Li, X., Kecorius, S., Groess, J., Shao, M., Wiedensohler, A., Zhang, Y., and Wang, T.:
701 Significant concentrations of nitryl chloride sustained in the morning: investigations of the
702 causes and impacts on ozone production in a polluted region of northern China, Atmospheric
703 Chemistry and Physics, 16, 14959-14977, 2016.
704 Tham, Y. J., Wang, Z., Li, Q., Wang, W., Wang, X., Lu, K., Ma, N., Yan, C., Kecorius, S.,
705 Wiedensohler, A., Zhang, Y., and Wang, T.: Heterogeneous N2O5 uptake coefficient and
706 production yield of ClNO2 in polluted northern China: roles of aerosol water content and
707 chemical composition, Atmospheric Chemistry and Physics, 18, 13155-13171, 2018.
708 Thornton, J. A., Kercher, J. P., Riedel, T. P., Wagner, N. L., Cozic, J., Holloway, J. S., Dube, W.
709 P., Wolfe, G. M., Quinn, P. K., Middlebrook, A. M., Alexander, B., and Brown, S. S.: A large
710 atomic chlorine source inferred from mid-continental reactive nitrogen chemistry, Nature, 464,
711 271-274, 2010.
712 Wang, H., Chen, J., and Lu, K.: Development of a portable cavity-enhanced absorption
713 spectrometer for the measurement of ambient NO 3 and N 2 O 5: experimental setup, lab
714 characterizations, and field applications in a polluted urban environment, Atmospheric
715 Measurement Techniques, 10, 1465, 2017a.
716 Wang, H., Lu, K., Guo, S., Wu, Z., Shang, D., Tan, Z., Wang, Y., Le Breton, M., Lou, S., Tang,
717 M., Wu, Y., Zhu, W., Zheng, J., Zeng, L., Hallquist, M., Hu, M., and Zhang, Y.: Efficient N2O5

718 uptake and NO3 oxidation in the outflow of urban Beijing, Atmospheric Chemistry and Physics,
719 18, 9705-9721, 2018.
720 Wang, H., Tang, M., Tan, Z., Peng, C., and Lu, K.: Atmospheric Chemistry of Nitryl Chloride,
721 Progress in Chemistry, 32, 1535-1546, 2020a.
722 Wang, T., Tham, Y. J., Xue, L., Li, Q., Zha, Q., Wang, Z., Poon, S. C. N., Dube, W. P., Blake, D.
723 R., Louie, P. K. K., Luk, C. W. Y., Tsui, W., and Brown, S. S.: Observations of nitryl chloride
724 and modeling its source and effect on ozone in the planetary boundary layer of southern China,
725 Journal of Geophysical Research-Atmospheres, 121, 2476-2489, 2016.
726 Wang, X., Hua, T., Zhang, C., Lang, L., and Wang, H.: Aeolian salts in Gobi deserts of the western
727 region of Inner Mongolia: Gone with the dust aerosols, Atmospheric Research, 118, 1-9, 2012.
728 Wang, X., Wang, H., Xue, L., Wang, T., Wang, L., Gu, R., Wang, W., Tham, Y. J., Wang, Z.,
729 Yang, L., Chen, J., and Wang, W.: Observations of N2O5 and ClNO2 at a polluted urban surface
730 site in North China: High N2O5 uptake coefficients and low ClNO2 product yields,
731 Atmospheric Environment, 156, 125-134, 2017b.
732 Wang, X., Jacob, D. J., Eastham, S. D., Sulprizio, M. P., Zhu, L., Chen, Q., Alexander, B., Sherwen,
733 T., Evans, M. J., Lee, B. H., Haskins, J. D., Lopez-Hilfiker, F. D., Thornton, J. A., Huey, G. L.,
734 and Liao, H.: The role of chlorine in global tropospheric chemistry, Atmospheric Chemistry and
735 Physics, 19, 3981-4003, 2019.
736 Wang, X., Jacob, D. J., Fu, X., Wang, T., Le Breton, M., Hallquist, M., Liu, Z., McDuffie, E. E.,
737 and Liao, H.: Effects of Anthropogenic Chlorine on PM2.5 and Ozone Air Quality in China,
738 Environmental Science & Technology, 54, 9908-9916, 2020b.
739 Wang, X., Jacob, D. J., Downs, W., Zhai, S., Zhu, L., Shah, V., Holmes, C. D., Sherwen, T.,
740 Alexander, B., Evans, M. J., Eastham, S. D., Neuman, J. A., Veres, P., Koenig, T. K., Volkamer,
741 R., Huey, L. G., Bannan, T. J., Percival, C. J., Lee, B. H., and Thornton, J. A.: Global
742 tropospheric halogen (Cl, Br, I) chemistry and its impact on oxidants, Atmos. Chem. Phys.
743 Discuss., 2021, 1-34, 2021.
744 Wang, Z., Wang, W. H., Tham, Y. J., Li, Q. Y., Wang, H., Wen, L., Wang, X. F., and Wang, T.:
745 Fast heterogeneous N2O5 uptake and ClNO2 production in power plant and industrial plumes
746 observed in the nocturnal residual layer over the North China Plain, Atmospheric Chemistry
747 and Physics, 17, 12361-12378, 2017c.
748 Wu, C., Zhang, S., Wang, G., Lv, S., Li, D., Liu, L., Li, J., Liu, S., Du, W., Meng, J., Qiao, L.,
749 Zhou, M., Huang, C., and Wang, H.: Efficient Heterogeneous Formation of Ammonium Nitrate
750 on the Saline Mineral Particle Surface in the Atmosphere of East Asia during Dust Storm
751 Periods, Environmental science & technology, 54, 15622-15630, 2020.
752 Young, C. J., Washenfelder, R. A., Edwards, P. M., Parrish, D. D., Gilman, J. B., Kuster, W. C.,
753 Mielke, L. H., Osthoff, H. D., Tsai, C., Pikelnaya, O., Stutz, J., Veres, P. R., Roberts, J. M.,
754 Griffith, S., Dusanter, S., Stevens, P. S., Flynn, J., Grossberg, N., Lefer, B., Holloway, J. S.,
755 Peischl, J., Ryerson, T. B., Atlas, E. L., Blake, D. R., and Brown, S. S.: Chlorine as a primary
756 radical: evaluation of methods to understand its role in initiation of oxidative cycles,
757 Atmospheric Chemistry and Physics, 14, 3427-3440, 2014.
758 Yu, C., Wang, Z., Xia, M., Fu, X., Wang, W., Tham, Y. J., Chen, T., Zheng, P., Li, H., Shan, Y.,
759 Wang, X., Xue, L., Zhou, Y., Yue, D., Ou, Y., Gao, J., Lu, K., Brown, S. S., Zhang, Y., and
760 Wang, T.: Heterogeneous N2O5 reactions on atmospheric aerosols at four Chinese sites:
761 improving model representation of uptake parameters, Atmos. Chem. Phys., 20, 4367-4378,
762 2020.

763 Zhang, H., Gu, W., Li, Y. J., and Tang, M.: Hygroscopic properties of sodium and potassium salts
764 as related to saline mineral dusts and sea salt aerosols, Journal of environmental sciences, 95,
765 65-72, 2020.
766 Zhang, X., Zhuang, G., Yuan, H., Rahn, K. A., Wang, Z., and An, Z.: Aerosol Particles from Dried
767 Salt-Lakes and Saline Soils Carried on Dust Storms over Beijing, Terrestrial Atmospheric and
768 Oceanic Sciences, 20, 619-628, 2009.
769 Zhang, X. X., Sharratt, B., Liu, L. Y., Wang, Z. F., Pan, X. L., Lei, J. Q., Wu, S. X., Huang, S. Y.,
770 Guo, Y. H., Li, J., Tang, X., Yang, T., Tian, Y., Chen, X. S., Hao, J. Q., Zheng, H. T., Yang, Y.
771 Y., and Lyu, Y. L.: East Asian dust storm in May 2017: observations, modelling, and its
772 influence on the Asia-Pacific region, Atmos. Chem. Phys., 18, 8353-8371, 2018.
773 Zheng, B., Tong, D., Li, M., Liu, F., Hong, C., Geng, G., Li, H., Li, X., Peng, L., Qi, J., Yan, L.,
774 Zhang, Y., Zhao, H., Zheng, Y., He, K., and Zhang, Q.: Trends in China's anthropogenic
775 emissions since 2010 as the consequence of clean air actions, Atmospheric Chemistry and
776 Physics, 18, 14095-14111, 2018.
777